

SELF-CONSISTENT RENORMALIZATION GROUP FLOW

Sen-Ben Liao^{1†} Chi-Yong Lin^{2,3‡} and Michael Strickland^{4*}

*Department of Physics¹
National Chung-Cheng University
Chia-Yi, Taiwan R. O. C.*

*Instituto De Fisica, Universidade De Sao Paulo²
C.P.66.318, CEP 05315-970, Sao Paulo, Brazil*

*Department of Physics³
National Dong-Hwa University
Hua-Lien, Taiwan R. O. C.*

and

*Department of Physics⁴
University of Washington
Seattle, WA 98195-1560 U.S.A.*

ABSTRACT

A self-consistent renormalization group flow equation for the scalar $\lambda\phi^4$ theory is analyzed and compared with the local potential approximation. The two prescriptions coincide in the sharp cutoff limit but differ with a smooth cutoff. The dependence of the critical exponent ν on the smoothness parameter and the field of expansion is explored. An optimization scheme based on the minimum sensitivity principle is employed to ensure the most rapid convergence of ν with the level of polynomial truncation.

CCU-TH-00-02

October 2000

† electronic address: senben@phy.ccu.edu.tw

‡ electronic address: lcyong@mail.ndhu.edu.tw

* electronic address: mike@phys.washington.edu

I. INTRODUCTION

In recent years there has been a resurging interest in using the exact renormalization group (ERG) formalism for investigating non-perturbative phenomena such as QCD in extreme conditions, dynamical chiral symmetry breaking and critical behavior of statistical systems. The ERG framework pioneered by Wilson [1], Wegner and Houghton [2], and Polchinski [3] was based on the concept of momentum-space blocking transformation under which the large momentum degrees of freedom are coarse-grained. Decreasing the cutoff systematically then leads to a nonlinear RG evolution equation which dictates how the effect of the irrelevant, short-distance modes can be incorporated into the low-energy effective blocked action.

The ERG flow equation may be derived starting from the generating functional for the connected Green's functions:

$$e^{W_k[J]} = \int D[\phi] e^{-\frac{1}{2}\phi \cdot C_k^{-1} \cdot \phi - S[\phi] + J \cdot \phi}, \quad (1.1)$$

where $C_k = \frac{\tilde{\rho}_{k,\sigma}(p)}{p^2(1-\tilde{\rho}_{k,\sigma}(p))}$ is an additive infrared (IR) cutoff, and $\tilde{\rho}_{k,\sigma}(p)$ is a smearing function which approaches $\Theta(p-k)$ as the smoothness parameter $\sigma \rightarrow \infty$. Upon varying the effective IR scale k infinitesimally followed by a Legendre transformation, $-W_k[J] + J \cdot \Phi = \tilde{S}_k[\Phi] + \frac{1}{2}\Phi \cdot C_k^{-1}\Phi$, $\Phi = \delta W_k/\delta J$, the RG equation for the blocked action $\tilde{S}_k[\Phi]$ is obtained as:

$$\begin{aligned} k \frac{\partial \tilde{S}_k}{\partial k} &= -\frac{1}{2} \text{Tr} \left[\frac{1}{C_k} \left(k \frac{\partial C_k}{\partial k} \right) \cdot \left(1 + C_k \cdot \frac{\delta^2 \tilde{S}_k}{\delta \Phi^2} \right)^{-1} \right] \\ &= -\frac{1}{2} \text{Tr} \left[\frac{1}{\tilde{\rho}_{k,\sigma}(1-\tilde{\rho}_{k,\sigma})} \left(k \frac{\partial \tilde{\rho}_{k,\sigma}}{\partial k} \right) \left(1 + \frac{\tilde{\rho}_{k,\sigma}}{p^2(1-\tilde{\rho}_{k,\sigma})} \frac{\delta^2 \tilde{S}_k}{\delta \Phi^2} \right)^{-1} \right]. \end{aligned} \quad (1.2)$$

The above equation has been derived and extensively analyzed [4] [5] [6]. Albeit being exact, it cannot be solved analytically and further approximation must be made for practical applications. Thus far the most reliable prescription which retains the original non-perturbative features has been the derivative expansion [7] where the blocked action is written as:

$$\tilde{S}_k[\Phi] = \int_x \left\{ \frac{Z_k(\Phi)}{2} (\partial_\mu \Phi)^2 + U_k(\Phi) + O(\partial^4) \right\}, \quad (1.3)$$

with $Z_k(\Phi)$ and $U_k(\Phi)$ being the wave-function renormalization constant and the blocked potential, respectively [8]. In the $O(\partial^0)$ order, the so-called Local Potential Approximation (LPA) [9] where $Z_k(\Phi)$ is taken to be unity, the RG evolution is characterized by

$$k \frac{\partial U_k(\Phi)}{\partial k} = \frac{1}{2} \int_p \left(k \frac{\partial \tilde{\rho}_{k,\sigma}(p)}{\partial k} \right) \frac{U''(\Phi)}{p^2 + \tilde{\rho}_{k,\sigma}(p) U''_k(\Phi)}. \quad (1.4)$$

The equation can now be readily solved by numerical methods [10].

A further approximation to the RG flow is to expand $U_k(\Phi)$ in powers of Φ and then truncate the series at some order M [11] [12]:

$$U_k(\Phi) = \sum_{n=1}^M \frac{g_{2n}(k)}{(2n)!} (\Phi - \Phi')^{2n}, \quad g_{2n}(k) = \frac{\partial^{2n} U_k}{\partial \Phi^{2n}} \Big|_{\Phi=\Phi'}, \quad (1.5)$$

thereby transforming the partial differential equation into a set of M coupled ordinary equations. Since the field expansion point Φ' is arbitrary, it may be chosen at the origin, the k -dependent minimum or any other non-vanishing field values [13]. Thus, polynomial truncation not only allows for a direct study of the flow of the coupling constants, numerical implementation is also greatly facilitated. However, the drawback of such truncated scheme is that it leads to spurious effects such as an oscillation in the value of the critical exponents and the appearance of complex eigenvalues at large M [4][12]. Therefore, it would be desirable to employ a prescription which ensures an unambiguous identification of the relevant fixed points as well as the convergence of physical quantities.

In Ref. [14] an optimization procedure based on the principle of minimum sensitivity was proposed for measuring the critical exponent ν . The parameter σ was dialed until it reached a value at which the minimum sensitivity condition $\frac{d\nu}{dM}|_{\sigma} = 0$ is satisfied. At the optimal σ , ν depends least sensitively on M due to the maximum suppression of the higher-order contributions, leading to a maximum rate of convergence for ν . An optimized scheme which retains only the relevant set of operators and the leading few irrelevant operators to characterize the RG flow can have non-trivial consequences in more complicated systems such as fermionic or gauge theories. In particular, the computation could be simplified enormously if certain classes of higher-order Feynman diagrams are suppressed.

In the present work we continue our search for an optimized RG prescription at the level of LPA. However, instead of following the conventional ERG approach as previously considered [14], we start from the one-loop contribution and introduce a “multiplicative” regulating smearing function $\tilde{\rho}_{k,\sigma}(p)$ in the momentum space integration:

$$\tilde{U}_k^{(1)}(\Phi) = \frac{1}{2} \int_p \tilde{\rho}_{k,\sigma}(p) \ln \left[1 + \frac{V''(\Phi)}{p^2} \right]. \quad (1.6)$$

The use of $\tilde{\rho}_{k,\sigma}(p)$ allows one to see clearly how each Feynman diagram is regularized. From the above equation, a self-consistent RG equation can be constructed by a differentiation with respect to k followed by the substitution $V''(\Phi) \rightarrow U''_k(\Phi)$ on the right-hand-side:

$$k \frac{\partial U_k(\Phi)}{\partial k} = \frac{1}{2} \int_p \left(k \frac{\partial \tilde{\rho}_{k,\sigma}(p)}{\partial k} \right) \ln \left[1 + \frac{U''_k(\Phi)}{p^2} \right]. \quad (1.7)$$

This procedure is analogous to the Schwinger-Dyson self-consistent improvement. The main focus of this paper is to illustrate how Eq. (1.7) can provide an alternative, viable prescription that retains the non-perturbative information contained in the original full RG equation for $\tilde{S}_k[\Phi]$. In particular, the convergence of physical quantities such as the critical exponents extracted using polynomial truncation will be demonstrated.

The organization of the paper is as follows. In Sec. II we briefly review the essential features of LPA and compare with the self-consistent RG equation, Eq. (1.7). The sharp cutoff limit of the RG flow is discussed in Sec. III and the dependence of the critical exponent ν on the field expansion point Φ_0 and the level of truncation M is also explored. We expand the potential about its k -dependent minimum, a prescription which does not respect the Z_2 symmetry of the original flow equation. Nevertheless, the resulting ν converges remarkably with increasing M up to $M = 26$. In Sec. IV the RG equations generated by smooth smearing functions are presented. Unlike the sharp cutoff case, singularities which resemble spontaneous symmetry breaking are present in the self-consistent integro-differential equation for the fixed-point solution $\bar{U}^*(\bar{\Phi})$ when employing a smooth cutoff. To overcome the complication we again make use of the non-invariant expansion and obtain numerical solutions for ν up to $M = 20$. Sec. V is reserved for summary and discussions. In Appendix A we summarize some detail associated with polynomial truncation of the sharp flow equation. The manner in which propagators are modified by LPA and the self-consistent RG schemes is discussed in Appendix B. In Appendix C we explore the large σ limit of the self-consistent RG.

II. LPA AND SELF-CONSISTENT RG

We first give a brief recapitulation of the basic features of LPA. The ERG equation can be constructed by introducing a smearing function $\rho_{k,\sigma}(x)$ which governs the coarse-graining procedure and k acts as an effective IR cutoff, separating the low- and the high-momentum modes. The propagator is modified as:

$$\Delta(p) = \frac{1}{p^2} \longrightarrow \Delta_{k,\sigma}(p) = \frac{1 - \rho_{k,\sigma}(p)}{p^2} = \frac{\tilde{\rho}_{k,\sigma}(p)}{p^2}, \quad (2.1)$$

where $\rho_{k,\sigma}(p) + \tilde{\rho}_{k,\sigma}(p) = 1$. In LPA where $Z_k(\Phi) = 1$ the evolution is characterized by the flow of $U_k(\Phi)$. For a generic smooth function $\rho_{k,\sigma}(p) = \Theta_\sigma(k, p)$, it is convenient to write $\Theta_\sigma(k, p) = t$ where $0 \leq t \leq 1$, and the reparameterization leads to

$$k \frac{dU_k(\Phi)}{dk} = \frac{S_d}{2} \int_{t(p=0)}^{t(p=\infty)} dt \frac{p^d(t) U''(\Phi)}{p^2(t) + (1-t)U_k''(\Phi)}. \quad (2.2)$$

Thus, by inverting $\rho_{k,\sigma}(p)$ for $p(t)$, the RG equation of $U_k(\Phi)$ is readily obtained.

Clearly, the evolution equation depends on the choice of the smearing function. While a sharp cutoff provides a well-defined boundary between the high (integrated) and the low (unintegrated) momentum modes and yields a partial differential equation, no clear separation exists for a smooth cutoff and the RG equation retains its integral-differential form. In principle, physical content extracted from solving the RG flow should not depend on the shape of the cutoff which merely reflects how the irrelevant degrees of freedom are integrated over. However, due to the approximation employed such dependence is explicitly present and the critical exponent ν exhibits a small dependence on σ [7]. The dependence may indicate that the effect of certain relevant operators has been neglected [15].

Within the framework of LPA, we see that Eq. (1.4) may also be obtained by a similar self-consistent “trick” starting from [16]:

$$\tilde{U}_k^{(1)}(\Phi) = \frac{1}{2} \int_p \ln \left[1 + \tilde{\rho}_{k,\sigma}(p) \frac{V''(\Phi)}{p^2} \right]. \quad (2.3)$$

This can be understood by noting that since we are now using an “exact” propagator, all the higher-order Feynman graphs that belong to the one-loop resummed class (e.g., daisy and super-daisy) are automatically incorporated. More generally, we may write:

$$\tilde{U}_k^{(1)}(\Phi) = \frac{1}{2} \int_p \ln \left[1 + \mathcal{P}_{k,\sigma}(p) \frac{V''(\Phi)}{p^2} \right], \quad (2.4)$$

with

$$\mathcal{P}_{k,\sigma}(p) \frac{1}{p^2} = \frac{\tilde{\rho}_{k,\sigma}(p)}{p^2} = \Delta_{k,\sigma}(p). \quad (2.5)$$

Here $\mathcal{P}_{k,\sigma}(p)$ acts as a projection operator on the massless propagator $1/p^2$ and turns it into an effective propagator $\tilde{\rho}_{k,\sigma}(p)/p^2$ which contains only the high momentum modes $p \gtrsim k$. For example, in the sharp limit one would have $\Delta_k(p) = \Theta(p - k)/p^2$.

Let us examine how the alternative, self-consistent RG prescription based on Eq. (1.6) differ from the usual LPA. First we note that since the coarse-graining procedure is initiated in the high-momentum regime where $V''(\Phi)/p^2 \ll 1$, Eq. (2.3) may be expanded as

$$\begin{aligned} \tilde{U}_k^{(1)}(\Phi) &= \frac{1}{2} \int_p \sum_{n=1}^{\infty} \frac{(-1)^{n+1}}{n} \left[\mathcal{P}_{k,\sigma}(p) \frac{V''(\Phi)}{p^2} \right]^n = \frac{1}{2} \int_p \sum_{n=1}^{\infty} \frac{(-1)^{n+1}}{n} \left[\tilde{\rho}_{k,\sigma} \frac{V''(\Phi)}{p^2} \right]^n \\ &= \frac{1}{2} \int_p \tilde{\rho}_{k,\sigma} \ln \left[1 + \frac{V''(\Phi)}{p^2} \right] + \frac{1}{2} \sum_{n=1}^{\infty} \frac{(-1)^{n+1}}{n+1} \int_p \tilde{\rho}_{k,\sigma} (1 - \tilde{\rho}_{k,\sigma}^n) \left(\frac{V''(\Phi)}{p^2} \right)^{n+1}. \end{aligned} \quad (2.6)$$

Differentiating both sides with respect to $\ln k$ and invoking the self-consistent prescription then leads to

$$\begin{aligned} k \frac{\partial U_k(\Phi)}{\partial k} &= \frac{1}{2} \int_p \left(k \frac{\partial \tilde{\rho}_{k,\sigma}(p)}{\partial k} \right) \ln \left[1 + \frac{U_k''(\Phi)}{p^2} \right] \\ &\quad + \frac{1}{2} \sum_{n=1}^{\infty} \frac{(-1)^{n+1}}{n+1} \int_p \left(k \frac{\partial \tilde{\rho}_{k,\sigma}(p)}{\partial k} \right) \left[1 - (n+1) \tilde{\rho}_{k,\sigma}^n(p) \right] \left(\frac{U_k''(\Phi)}{p^2} \right)^{n+1}. \end{aligned} \quad (2.7)$$

In the first term of the equation above one finds a complete factorization between the running of the scale k and the Φ dependence. This is the equation which we shall focus on in the subsequent sections. The second term, representing the difference between the self-consistent RG and the LPA, can also be written as:

$$\Delta U_k(\Phi) = \frac{S_d}{2} \int_{t(p=0)}^{t(p=\infty)} dt p^d(t) \left\{ \frac{U_k''(\Phi)}{p^2(t) + (1-t)U_k''(\Phi)} - \ln \left[p^2(t) + U_k''(\Phi) \right] \right\}. \quad (2.8)$$

From Eq. (2.6) or (2.8), we see that the two RG schemes coincide when $\tilde{\rho}_{k,\sigma}(p) \rightarrow 1$ or 0. That is, $\Delta U_k(\Phi) = 0$ when $\mathcal{P}_{k,\sigma}^2(p) = \mathcal{P}_{k,\sigma}(p)$ or $\tilde{\rho}_{k,\sigma}^2(p) = \tilde{\rho}_{k,\sigma}(p)$. However, this holds only for the trivial case of a sharp cutoff; smooth cutoffs such as $\tilde{\rho}_{k,b}(p) = 1 - e^{-a(p/k)^b}$ and $\tilde{\rho}_{k,m}(p) = (p/k)^m/(1 + (p/k)^m)$, on the other hand, give a small deviation for large m and b in the regime $p/k \gg 1$.

The salient feature of our approach is that once the perturbative results are known, they can be readily transformed into the corresponding self-consistent RG equations. Generalization to higher order derivative expansion can be achieved with ease. For example, at order $O(\partial^2)$, we have:

$$k \frac{\partial U_k(\Phi)}{\partial k} = \frac{1}{2} \int_p \left(k \frac{\partial \tilde{\rho}_{k,\sigma}(p)}{\partial k} \right) \ln \left[1 + \frac{U_k''(\Phi)}{Z_k(\Phi)p^2} \right], \quad (2.9)$$

and [17] [18]

$$\begin{aligned} k \frac{\partial Z_k}{\partial k} = & \int_p \left(k \frac{\partial \tilde{\rho}_{k,\sigma}(p)}{\partial k} \right) \left\{ \frac{Z_k''}{Z_k p^2 + U_k''} - 2Z_k' \frac{Z_k' p^2 + U_k'''}{(Z_k p^2 + U_k'')^2} - \frac{p^2}{d} \frac{(Z_k')^2}{(Z_k p^2 + U_k'')^2} \right. \\ & \left. + \frac{4p^2}{d} Z_k Z_k' \frac{Z_k' p^2 + U_k'''}{(Z_k p^2 + U_k'')^3} + Z_k \frac{(Z_k' p^2 + U_k''')^2}{(Z_k p^2 + U_k'')^3} - \frac{4p^2}{d} Z_k^2 \frac{(Z_k' p^2 + U_k''')^2}{(Z_k p^2 + U_k'')^4} \right\}. \end{aligned} \quad (2.10)$$

We comment that the above prescription, being reminiscent to the Schwinger-Dyson approach, has been widely employed to treat more complicated issues such as the effective quark propagator [19] and dynamical chiral symmetry breaking in gauge theories [20]. One great advantage here is that, unlike the exact RG approach, the flow for $Z_k(\Phi)$ is completely analytic, even in the sharp cutoff limit, and the numerical algorithm can be readily implemented. Incorporating the effect of $Z_k(\Phi)$ with the above approach has been shown to improve the accuracy of ν [21]. In what follows we shall set $Z_k(\Phi) = 1$ ($\eta = 0$) for simplicity.

Although we shall mainly be concerned with smearing functions that approach a step function as $\sigma \rightarrow \infty$ in our self-consistent RG scheme, other type of regularization can also be utilized. For example, one could choose the smearing function to be of the Pauli-Villars type:

$$\tilde{\rho}_k(p) = \left(\frac{\Lambda^2}{p^2 + \Lambda^2} \right)^{d/2} - \left(\frac{k^2}{p^2 + k^2} \right)^{d/2}. \quad (2.11)$$

In a similar manner, the spirit of the dimensional regularization can also be encapsulated by using $\tilde{\rho}_\epsilon(p) = d^{-\epsilon} p / (2\pi)^{-\epsilon}$ in integer d ; with $\lambda \rightarrow \lambda \mu^\epsilon$, the RG flow is described by μ , the renormalization point.

III. SELF-CONSISTENT RG - SHARP CUTOFF

Before considering smooth cutoffs, it is instructive to first review the sharp cutoff results [14]. In order to recover this limit, caution must be taken to invert $t = \Theta(1 - z)$.

Here it must be interpreted that t changes *continuously* from 1 to 0 at $z = 1$, thereby leading to [4]:

$$\left[k \frac{\partial}{\partial k} - \frac{1}{2} (d-2) \bar{\Phi} \frac{\partial}{\partial \bar{\Phi}} + d \right] \bar{U}_k(\bar{\Phi}) = - \int_0^1 dt \ln [1 + \bar{U}_k''(\Phi)] = -\ln [1 + \bar{U}_k''(\Phi)], \quad (3.1)$$

where $\bar{U}_k(\bar{\Phi}) = \zeta^2 k^{-d} U_k(\Phi)$, $\bar{\Phi} = \zeta k^{-(d-2)/2} \Phi$, with $\zeta = \sqrt{2/S_d} = \sqrt{(4\pi)^{d/2} \Gamma(d/2)}$. The fixed-point solution is given by

$$-\frac{1}{2} (d-2) \bar{\Phi} \bar{U}^{*'} + d \bar{U}^* = -\ln [1 + \bar{U}^{*''}], \quad (3.2)$$

with $U^{*'}(0) = 0$ from reflection symmetry.

However, it has been pointed out that only certain values of $\bar{g}_0^* = \bar{U}^*(0) = -\ln(1 + \bar{g}_2^*)/d$ can lead to physically meaningful solutions [4][11]; in all other cases a singularity of the form $\bar{U}^* \sim \ln(\bar{\Phi}_c - \bar{\Phi})$ will be encountered and the potential becomes complex beyond some critical value $\bar{\Phi}_c$. In $d = 3$, only two solutions have been found; the first one is $\bar{g}_0^* = 0$ which corresponds to the trivial Gaussian fixed point and the second one, $\bar{g}_0^* = 0.206343 \equiv s_0$ (or $\bar{g}_2^* = -0.461533 \equiv s$), the Wilson-Fisher. The qualitative feature of the fixed-point solutions is illustrated in Fig. 1.

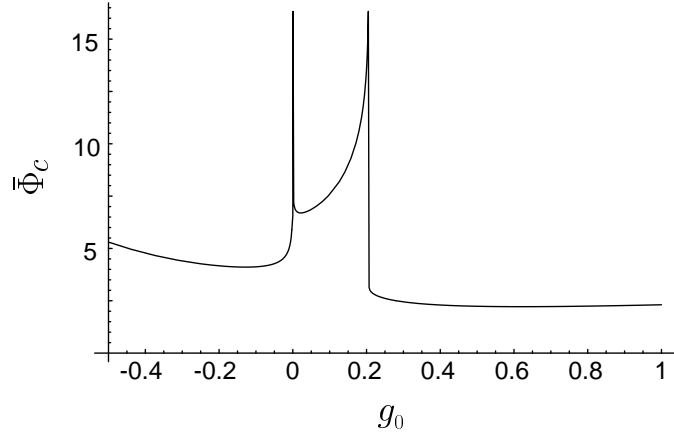


Figure 1. Singularity $\bar{\Phi}_c$ as a function of g_0 in $d=3$. Notice that there are only two physical solutions, one for the Gaussian and the other one for the Wilson-Fisher fixed point.

As we mentioned in the Introduction, instead of solving the full flow equation, we may expand $\bar{U}_k(\bar{\Phi})$ in powers of $\bar{\Phi}$ and terminate the series at $\bar{\Phi}^{2M}$, thereby turning the nonlinear partial differential equation into a set of M coupled ordinary differential equations. We consider below expansion schemes that are both Z_2 -invariant and non-invariant.

a. invariant expansion

The simplest invariant polynomial expansion of $\bar{U}_k(\bar{\Phi})$ can be carried out around $\bar{\Phi} = 0$, as in Eq. (1.5). The $\bar{\beta}$ functions, $\bar{\beta}_n = k\partial\bar{g}_n/\partial k$, can be written as:

$$\begin{aligned}\bar{\beta}_2 &= -2\bar{g}_2 - \bar{G}_4, \\ \bar{\beta}_4 &= -\epsilon\bar{g}_4 - (-3\bar{G}_4^2 + \bar{G}_6), \\ \bar{\beta}_6 &= (2d - 6)\bar{g}_6 - (30\bar{G}_4^3 - 15\bar{G}_4\bar{G}_6 + \bar{G}_8), \dots\end{aligned}\tag{3.3}$$

where $\bar{G}_n = \bar{g}_n/(1 + \bar{g}_2)$ [22], and the fixed points can now be located by setting $\bar{\beta}_n = 0$ for all n . If only \bar{g}_2 and \bar{g}_4 are kept, we find, besides the trivial fixed point $(\bar{g}_2^*, \bar{g}_4^*) = (0, 0)$, an additional Wilson-Fisher fixed point $(\bar{g}_2^*, \bar{g}_4^*) = (-\frac{\epsilon}{6+\epsilon}, \frac{12\epsilon}{(6+\epsilon)^2})$. Linearizing the flow about the above fixed point, the eigenvalues can easily be found to be $[(-3 + 2\epsilon) \pm \sqrt{9 + 6\epsilon + 7\epsilon^2}]/3$, or $(-1 \pm \sqrt{22})/3$ for $\epsilon = 1$. By our convention, the largest *negative* eigenvalue corresponds to the inverse of the critical exponent $1/\nu$. Thus, we have $\nu \approx 0.5272$ at $M = 2$. We remark that in the spirit of the conventional ϵ -expansion where ϵ is first taken to be “small,” the matrix element $\partial\bar{\beta}_4/\partial\bar{g}_2$ which is $O(\epsilon^2)$ is discarded, and $\nu = 0.6$ instead [23]. Thus, when characterizing the flow by powers of $\bar{\Phi}$, there is a reshuffling of contributions from the ϵ series.

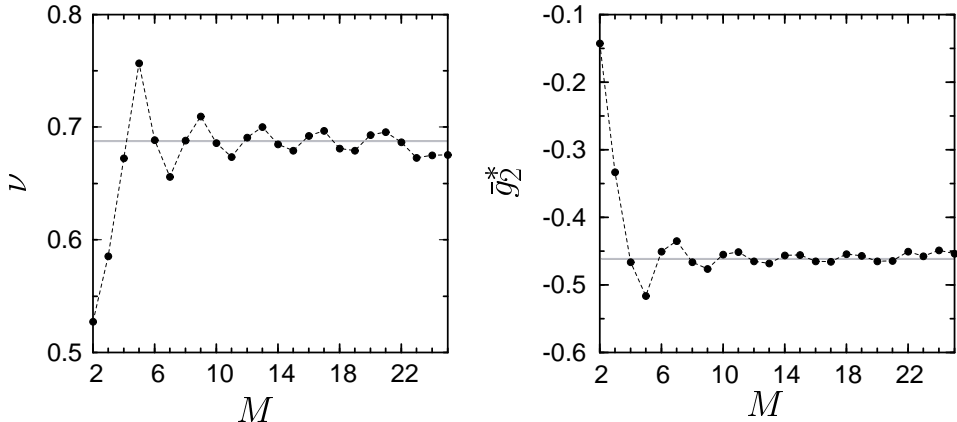


Figure 2. Oscillation of critical exponent ν and g_2^* as a function of M .

However, it is well-known that ν obtained via polynomial truncation with a sharp cutoff generally does not converge but oscillates with M , as depicted in Fig. 2. We find that at $M = 22$ an additional relevant direction is generated; and as M is further increased, more spurious solutions are found and the identification of the Wilson-Fisher fixed point becomes ambiguous. The oscillation in ν is intimately linked to the oscillation in \bar{g}_2^* and the cause is related to the singular structure of the non-truncated fixed point potential $\bar{U}^*(\bar{\Phi})$ on the complex plane [4]; namely, the asymptotic behavior is dominated by a pole $\bar{\Phi}_c = |\bar{\Phi}_c|e^{i\theta_c}$ having $\theta_c \approx \pm\pi/2$ that gives rise to an approximate four-fold periodicity. Such truncation dependence is not unexpected since the fixed point(s) one identifies at each order is only approximate and not the *true* Wilson-Fisher fixed point; therefore, the would-be irrelevant set of operators will continue to evolve, leading to the M dependence

of physical quantities. In order to improve the convergence of ν in polynomial truncation, Aoki *et al* has carried out an expansion about a Z_2 -invariant field $\bar{\chi}_0 = \bar{\Phi}_0^2/2$ [13]:

$$\bar{U}_k(\bar{\chi}) = \sum_{n=0}^M \frac{c_n(k)}{n!} (\bar{\chi} - \bar{\chi}_0)^n, \quad c_n(k) = \bar{U}_k^{(n)}(\chi_0) = \frac{\partial^n \bar{U}_k}{\partial \bar{\chi}^n} \Big|_{\bar{\chi}=\bar{\chi}_0}. \quad (3.4)$$

The convergence has been found to improve dramatically. A more thorough discussion of this expansion scheme is presented in Appendix A.

b. non-invariant expansion

Alternatively, one may expand the potential around some non-vanishing $\bar{\Phi}'$:

$$\bar{U}_k(\bar{\Phi}) = \sum_{n=0}^M \frac{\hat{g}_n(k)}{n!} (\bar{\Phi} - \bar{\Phi}')^n, \quad \hat{g}_n(k) = \bar{U}_k^{(n)}(\Phi') = \frac{\partial^n \bar{U}_k}{\partial \bar{\Phi}^n} \Big|_{\bar{\Phi}=\bar{\Phi}'}. \quad (3.5)$$

Here the presence of odd powers of $\bar{\Phi}$ will explicitly break the Z_2 symmetry. However, this novel prescription becomes particularly useful when spontaneous symmetry breaking takes place, or when the running mass parameter $\bar{g}_2(k)$ is still negative during the RG evolution. It also allows us to monitor the flow around $\bar{\Phi}'$ instead of the origin.

Choosing $\bar{\Phi}' = \bar{\Phi}_0$, the k -dependent minimum and using Eq. (3.5), we obtain

$$\begin{aligned} \dot{\bar{\Phi}}_0 &= -(1 - \frac{\epsilon}{2})\bar{\Phi}_0 + \hat{G}_3/\hat{g}_2, \\ \dot{\hat{g}}_2 &= \hat{g}_3 \dot{\bar{\Phi}}_0 - 2\hat{g}_2 + (1 - \frac{\epsilon}{2})\bar{\Phi}_0 \hat{g}_3 + (\hat{G}_3^2 - \hat{G}_4), \\ \dot{\hat{g}}_3 &= \hat{g}_4 \dot{\bar{\Phi}}_0 - (1 + \frac{\epsilon}{2})\hat{g}_3 + (1 - \frac{\epsilon}{2})\bar{\Phi}_0 \hat{g}_4 + (-2\hat{G}_3^3 + 3\hat{G}_3 \hat{G}_4 - \hat{G}_5), \\ \dot{\hat{g}}_4 &= \hat{g}_5 \dot{\bar{\Phi}}_0 - \epsilon \hat{g}_4 + (1 - \frac{\epsilon}{2})\bar{\Phi}_0 \hat{g}_5 + (6\hat{G}_3^4 - 12\hat{G}_3^2 \hat{G}_4 + 3\hat{G}_4^2 + 4\hat{G}_3 \hat{G}_5 - \hat{G}_6), \dots \end{aligned} \quad (3.6)$$

where $\hat{G}_n = \frac{\hat{g}_n}{1+\hat{g}_2}$. At the fixed point where $\dot{\bar{\Phi}}_0$ vanishes, we have $\bar{\Phi}_0^* = \frac{2\hat{g}_3^*}{(2-\epsilon)\hat{g}_2^*(1+\hat{g}_2^*)}$. When solving the coupled equations $\dot{\hat{g}}_n = 0$ to locate the fixed points, one finds that the number of spurious solutions again increases with M . Moreover, due to the loss of Z_2 symmetry, the Wilson-Fisher fixed point no longer has just one relevant eigen-direction, as would be in the Z_2 -symmetric case.

The new Wilson-Fisher fixed point which dictates the critical behavior of the Ising universality class satisfies the following conditions: (i) all the fixed-point coupling constants \hat{g}_n^* 's are real, (ii) the extremum of $\bar{U}^*(\bar{\Phi})$ is close to $\bar{\Phi}_0^* = 1.9287$, the field value obtained from solving the full non-truncated LPA equation, and (iii) at $M = 2j$ ($j > 2$) there are $\ell = j+1$ relevant eigen-directions which, by our convention, have negative real part for the eigenvalues. Let us see how the above criteria work. First we note that $\bar{g}_2^* < 0$ for $M < 6$, an indication that $\bar{\Phi}_0$ is a local maximum. At $M = 4$ there are only three non-trivial solutions $(\bar{g}_2^*, \bar{g}_3^*, \bar{g}_4^*) = (-\frac{1}{7}, 0, \frac{12}{49})$ and $(-0.4125, \pm 0.2327, 0.4456)$, with the first being the usual Z_2 -symmetric solution at $\bar{\Phi}_0 = 0$. We choose the asymmetric solution with $\bar{g}_3^* < 0$, which yields $\bar{\Phi}_0 = 1.9203$ and $\nu = 0.4229$. For $M \geq 6$, the extremum becomes a local

minimum and we have $\ell = j + 1$. This is due to the fact that the fields that break the Z_2 symmetry remain relevant throughout. In addition, there are two more coupling constants, \bar{g}_2^* and \bar{g}_4^* , which are relevant by power counting. For example, at $M = 10$ the relevant set should be $\{\bar{g}_2^*, \bar{g}_3^*, \bar{g}_4^*, \bar{g}_5^*, \bar{g}_7^*, \bar{g}_9^*\}$, i.e., $\ell = 6$. Note that the classification of operators around the trivial Gaussian fixed point is still based on the counting of their canonical dimensions $[\bar{g}_n] = d - n(\frac{d}{2} - 1)$.

The fixed-point potential $\bar{U}^*(\bar{\Phi})$ is plotted in Fig. 3 as a function of $\bar{\Phi}$ for various M . Due to the Z_2 asymmetry and the choice $\bar{\Phi}_0 > 0$ as the expansion point, only $\bar{U}^*(\bar{\Phi})$ with positive $\bar{\Phi}$ is tracked. We note that the approximation first improves with increasing M and nearly coincides with the full non-truncated potential at $M = 20$. Incidentally this is the order at which the term linear in $\bar{\Phi}$ that represents the leading symmetry-breaking contribution is minimized. However, beyond $M = 20$ the potential begins to deviate away from the non-truncated LPA solution. At $M = 28$ a sensible result can be obtained only by choosing a complex eigenvalue. The remarkable convergence of ν with increasing M up to $M = 26$ is depicted in Fig. 4. Note that in the Z_2 -invariant polynomial truncation scheme, depending on the point of expansion, ν is found to converge to or oscillate about 0.689, which is the value obtained by solving the non-truncated LPA equation. On the other hand, our non-invariant prescription gives 0.649 for a large range of M . Such discrepancy is not unexpected since the symmetry of fixed points for the Ising universality class differs in the two cases. It is interesting also to note that the result is very close to the value 0.651 obtained via the optimization procedure in which the most optimal smoothness parameter is sought to achieve minimum sensitivity [14].

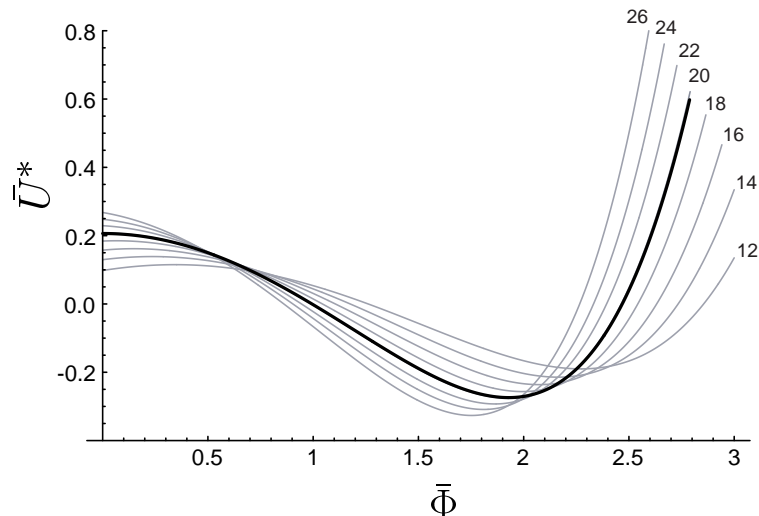


Figure 3. Fixed-point potential $\bar{U}^*(\bar{\Phi})$ obtained by polynomial truncation. Exact LPA solution is shown as solid black line. The agreement with the full LPA solution first improves with increasing M and nearly coincides at $M=20$.

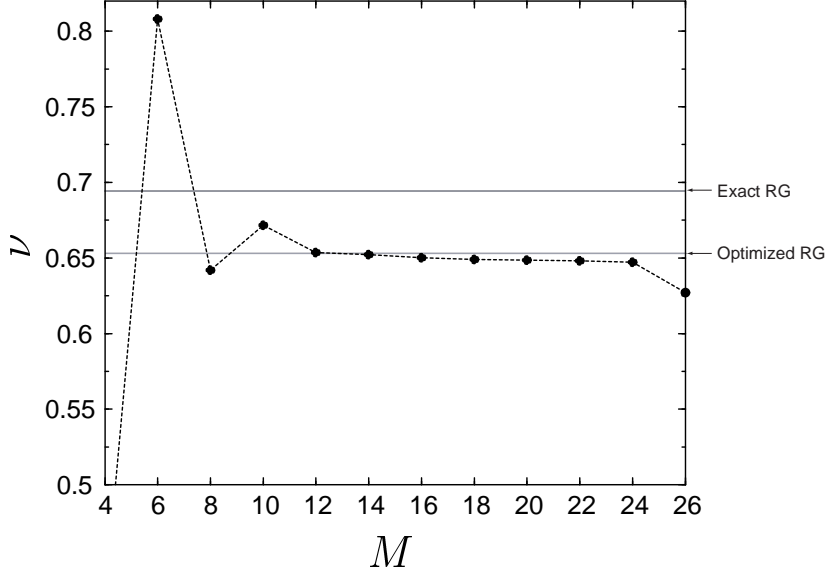


Figure 4. Critical exponent ν as a function of M obtained by an non-invariant expansion of $\bar{U}^*(\bar{\Phi})$ about the minimum $\bar{\Phi}_0$.

We comment that besides the origin or the k -dependent minimum $\bar{\Phi}_0$, in principle $\bar{\Phi}'$ can be arbitrarily chosen. However, the rate of convergence is closed linked to the choice of $\bar{\Phi}'$. Aoki *et al* has shown that expanding the sharp cutoff RG equation for $\bar{U}^*(\bar{\Phi})$ about the minimum, $\bar{\Phi}_0$, yields a larger radius of convergence compared to at the origin [13]. In fact, it leads to the exact solution in the large N limit. Thus, when expanding about the minimum $\bar{\Phi}_0$, a sharp cutoff smearing function with $\sigma \rightarrow \infty$ would be the optimal “smoothness” that satisfies the minimum sensitivity principle, as we shall see in the next Section.

IV. SELF-CONSISTENT RG - SMOOTH CUTOFFS

In this Section we examine the fixed-point potential $\bar{U}^*(\bar{\Phi})$ obtained via polynomial truncation with smooth cutoffs. Unlike the sharp cutoff case, the RG flow is characterized by the following (dimensionless) integro-differential equation:

$$\begin{aligned} \left[k \frac{\partial}{\partial k} - \frac{1}{2} (d-2) \bar{\Phi} \frac{\partial}{\partial \bar{\Phi}} + d \right] \bar{U}_k(\bar{\Phi}) &= \int_0^\infty dz z^{d-1} \left(k \frac{\partial \tilde{\rho}_{k,\sigma}}{\partial k} \right) \ln \left[z^2 + \bar{U}_k''(\bar{\Phi}) \right] \\ &= - \int_0^1 dt z^d(t) \ln \left[z^2(t) + \bar{U}_k''(\bar{\Phi}) \right]. \end{aligned} \quad (4.1)$$

The smearing functions are chosen in such a way that the conditions $t(z=0) = 1$ and $t(z=\infty) = 0$ are always satisfied. However, we shall find that within a certain range of k in the smooth case the running mass parameter $\bar{g}_2(k)$ (as well as \bar{g}_2^*) are negative quantities and singularity is encountered in $\bar{\beta}_n$ as the denominator $z^2(t) + \bar{U}_k''(\bar{\Phi})$ goes to zero.

The reason why such singularity is absent in the sharp cutoff but present in the smooth cutoff for self-consistent RG can be understood from the manner in which the large momentum modes are eliminated. In the case of exact RG a sharp cutoff provides a clear separation between the integrated ($z \equiv p/k > 1$) and the unintegrated modes ($z \equiv p/k < 1$). With a negative mass curvature $\bar{g}_2^* = s \approx -0.461533$ (in unit of k) for the non-truncated potential, the integration is completely analytic because the condition $1 + s > 0$ is always satisfied in the denominator. However, in the self-consistent RG formulation no sharp boundary exists for a smooth cutoff and for any finite σ the range of the z integration is stretched from zero to infinity. Therefore, singularity sets in when $z^2 + s \leq 0$. The situation confronted here actually resembles that of spontaneous symmetry breaking where the potential is also double-welled. However, we emphasize that $\bar{U}^*(\bar{\Phi})$ describes a scale-invariant theory in the symmetric phase; as we integrate down to $k = 0$ in the *dimensionful* RG equation, the potential will become single-welled with a unique minimum at the origin [10]. True symmetry breaking is marked by $\lim_{k \rightarrow 0} g_2(k) < 0$. Notice that the integration with a smooth cutoff would be completely analytic had the LPA prescription been employed; the difference between the two schemes may be attributed to the manner in which the propagators are modified. The details are further discussed in Appendix B.

To overcome the difficulty associated with the divergence near $z = \sqrt{-\bar{g}_2^*}$, we expand the potential about a non-zero minimum $\bar{\Phi}_0$ where $\bar{U}''(\bar{\Phi}_0) = \hat{g}_2 > 0$, as in Eq. (3.5). In analogy to Eq. (3.6), we have, for the smooth case:

$$\begin{aligned} \dot{\bar{\Phi}}_0 &= -\left(1 - \frac{\epsilon}{2}\right)\bar{\Phi}_0 + \int_0^1 z^d(t) \hat{\mathcal{G}}_3/\hat{g}_2, \\ \dot{\hat{g}}_2 &= \hat{g}_3 \dot{\bar{\Phi}}_0 - 2\hat{g}_2 + \left(1 - \frac{\epsilon}{2}\right)\bar{\Phi}_0 \hat{g}_3 + \int_0^1 dt z^d(t) (\hat{\mathcal{G}}_3^2 - \hat{\mathcal{G}}_4), \\ \dot{\hat{g}}_3 &= \hat{g}_4 \dot{\bar{\Phi}}_0 - \left(1 + \frac{\epsilon}{2}\right)\hat{g}_3 + \left(1 - \frac{\epsilon}{2}\right)\bar{\Phi}_0 \hat{g}_4 + \int_0^1 dt z^d(t) (-2\hat{\mathcal{G}}_3^3 + 3\hat{\mathcal{G}}_3 \hat{\mathcal{G}}_4 - \hat{\mathcal{G}}_5), \\ \dot{\hat{g}}_4 &= \hat{g}_5 \dot{\bar{\Phi}}_0 - \epsilon \hat{g}_4 + \left(1 - \frac{\epsilon}{2}\right)\bar{\Phi}_0 \hat{g}_5 + \int_0^1 dt z^d(t) (6\hat{\mathcal{G}}_3^4 - 12\hat{\mathcal{G}}_3^2 \hat{\mathcal{G}}_4 + 3\hat{\mathcal{G}}_4^2 + 4\hat{\mathcal{G}}_3 \hat{\mathcal{G}}_5 - \hat{\mathcal{G}}_6), \end{aligned} \tag{4.2}$$

where $\hat{\mathcal{G}}_n = \frac{\hat{g}_n}{z^2(t) + \hat{g}_2}$. The absence of linear term implies $\bar{\Phi}_0 = \frac{2}{(2-\epsilon)\hat{g}_2} \int_0^1 dt z^d(t) \hat{\mathcal{G}}_3$. The flow of $\bar{\Phi}_0$ is connected with that of \hat{g}_n with n odd; naturally all odd coupling constants vanish when $\bar{\Phi}_0 = 0$.

Consider the two smooth representations:

$$\rho_{k,b}(p) = e^{-a(p/k)^b} \longrightarrow z(t) = \left(\frac{-\ln t}{a}\right)^{1/b}, \tag{4.3}$$

and

$$\rho_{k,m}(p) = [1 + (p/k)^m]^{-1} \longrightarrow z(t) = \left(\frac{1}{t} - 1\right)^{1/m}. \tag{4.4}$$

We choose $a = \ln 2$ so that $\rho_{k,b}(p = k) = 1/2$ and the smoothness of the cutoff is controlled by a single parameter b [24]. From Figures 5 and 6 depicted below, it is clear that

the sharper the cutoff the more rapid the convergence for ν in the polynomial truncation scheme. That is, $m, b = \infty$ is the optimal value at which the minimum sensitivity condition $\frac{d\nu}{dM}|_{b,m} = 0$ is met. As $b(m)$ is decreased, ν oscillates with increasing amplitude. Comparing the two figures, one also notices a smaller oscillation amplitude for the exponential cutoff.

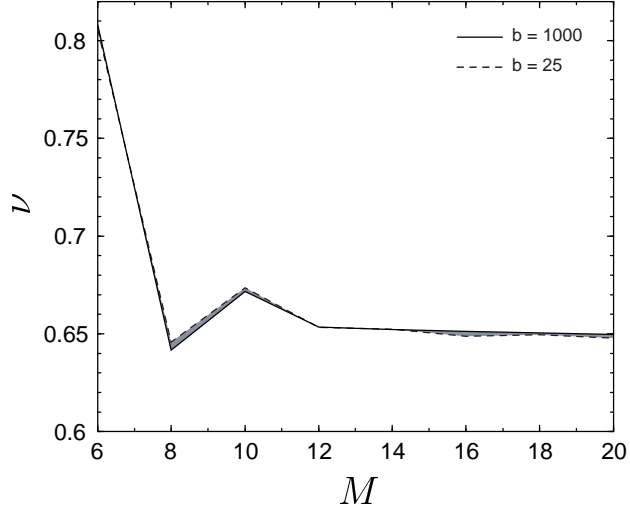


Figure 5. Critical exponent ν as a function of b for various M . The optimal smearing function corresponds to a sharp cutoff with $b=\infty$. As b is decreased, ν begins to oscillate with increasing amplitude.

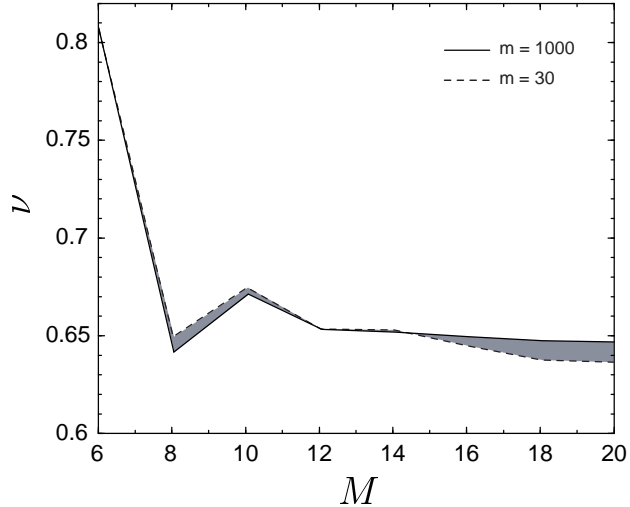


Figure 6. Critical exponent ν as a function of m for various M . The “optimal” smoothness here again is $m=\infty$.

We emphasize again that the optimal smoothness σ obtained from the minimum sensitivity principle generally depends on the model under study as well as the approximation employed. While a sharp cutoff is the optimal smoothness when $\bar{\Phi}'$ is chosen to be the minimum $\bar{\Phi}_0$ of the potential, for an arbitrary $\bar{\Phi}'$, the optimal σ which satisfies the minimum

sensitivity condition would correspond to a smooth cutoff. On the other hand, a sharp cutoff yields a rather poor convergence for $\bar{\Phi}' = 0$. A general criterion of finding the optimal σ can be found by analyzing the massless blocked propagator $\Delta_\sigma(z) = 1/P_\sigma^2(z) = \tilde{\rho}_{k,\sigma}/z^2$, as has been recently shown by Litim (see Appendix B) [15].

V. SUMMARY AND DISCUSSIONS

In the present work we introduced a self-consistent RG prescription starting from the one-loop perturbative expression. Our self-consistent equation coincides with LPA in the sharp cutoff limit but differs with a smooth cutoff. The advantage of this novel approach is that the perturbative independent-mode results can be readily “dressed” into a set of coupled non-linear RG equations. Complication arising from taking the sharp cutoff limit in the derivative expansion can also be avoided completely.

Due to the absence of a sharp boundary in the momentum integration in the smooth cases, a singularity is encountered in solving the truncated self-consistent equations, as the inverse propagator $z^2 + \bar{g}_2^*$ vanishes. We circumvent this difficulty by expanding $\bar{U}^*(\bar{\Phi})$ about its minimum $\bar{\Phi}_0$ where $\hat{g}_2^* > 0$. Such expansion is non-invariant since it contains odd powers of $\bar{\Phi}$ that destroys Z_2 symmetry. The system remains, however, in the symmetric phase; as we integrate down to $k = 0$ in the dimensionful flow equation, the moving minimum $\Phi_0(k)$ vanishes. Nevertheless, the formal equivalence provides a useful tool for exploring systems in the state of broken symmetry.

In the absence of Z_2 symmetry, the physical, Wilson-Fisher fixed point which governs the critical behavior of the Ising universality class may be readily identified from the following conditions: (i) all the coupling constants \bar{g}_n^* ’s are real; (ii) the potential has an extremum close to $\bar{\Phi}_0^* = 1.9287$, the value obtained without truncation; and (iii) the number of relevant eigen-directions is $j + 1$ for $M = 2j$ ($j > 2$). Having identified the fixed point, the exponent ν is extracted from the truncated polynomial series. As shown in Sec. III, when a sharp cutoff is employed, ν oscillates with M when $\bar{U}^*(\bar{\Phi})$ is expanded about $\bar{\Phi} = 0$. On the other hand, the convergence improves dramatically in the non-invariant expansion about the minimum $\bar{\Phi}_0$. We truncated the series at $M = 28$ where the eigenvalues become complex. From Figure 4, we see that with increasing M the series converges rapidly to approximately $\nu = 0.649$, which differs from the full LPA solution 0.689. The discrepancy may be attributed to the difference in the symmetry of the two approaches. In Sec. IV where smooth cutoffs are considered, one finds that the amplitude of oscillation grows with a smaller σ , and the rate of convergence decreases. Thus, the sharp cutoff is the “optimal” smearing function for the self-consistent RG expanded about the minimum $\bar{\Phi}_0$. Indeed, the minimal sensitivity condition $\frac{d\nu}{dM}|_\sigma = 0$ is reached as $\sigma \rightarrow \infty$.

The results obtained in this paper demonstrates that when solving the truncated RG equations for $\bar{U}_k(\bar{\Phi})$, the convergence of physical quantities is strongly influenced by two factors: (i) the expansion point $\bar{\Phi}_0$, and (ii) the smoothness parameter σ in the smearing function $\tilde{\rho}_{k,\sigma}(p)$. An optimal choice of $\bar{\Phi}_0$, usually the minimum of $\bar{U}_k(\bar{\Phi})$, yields the largest radius of convergence in the expansion [13]. However, when $\bar{\Phi}_0$ is not optimal, one can fine-tune σ so that physical quantities such as ν would exhibit minimal sensitivity on the order of truncation M .

The optimization prescription presented here can be readily extended to more complicated systems. Polynomial truncation applied to models with fermionic interaction can be considered [25]. A self-consistent RG prescription with a smooth cutoff can also be formulated via the operator cutoff regularization in the proper-time space [21] [26]. In order to test the success of our self-consistent RG scheme, the effect of wave function renormalization constant $Z_k(\bar{\Phi})$ must be incorporated. The results will be reported in the forthcoming publication [27].

ACKNOWLEDGMENTS

S.-B. L. is grateful to D. Litim, J. Polonyi and Y.-C. Tsai for valuable discussions and the hospitality of the Institute for Nuclear Theory, University of Washington during his visit. This work is supported in part by funds provided by the National Science Council of Taiwan under contract #NSC-89-2112-M-194-005 and by the United States Department of Energy Grant DG-FG03-97-ER41014. C-Y. Lin was partially supported by FAPESP, Brazil.

APPENDIX A: SHARP RG FLOW BY POLYNOMIAL TRUNCATION

In this Appendix, we provide some detail of the RG behavior near the Wilson-Fisher fixed point, based on the polynomial truncation. The evolution equation obtained with a sharp cutoff reads, in $d = 3$:

$$\dot{\bar{U}}_k(\bar{\Phi}) - \frac{1}{2}\bar{\Phi}\bar{U}'_k(\bar{\Phi}) + 3\bar{U}_k(\bar{\Phi}) = -\ln \left[1 + \bar{U}''_k(\bar{\Phi}) \right]. \quad (\text{A.1})$$

There are several ways to obtain an approximate solution to the fixed-point equation. We summarize two schemes below:

1. expansion about $\bar{\Phi} = 0$:

Here we assume the potential to be of the form:

$$\bar{U}_k(\bar{\Phi}) = \sum_{n=1}^M \frac{\bar{g}_{2n}(k)}{(2n)!} \bar{\Phi}^{2n}, \quad \bar{g}_{2n}(k) = \bar{U}_k^{(2n)}(0) = \frac{\partial^{2n}\bar{U}_k}{\partial\bar{\Phi}^{2n}} \Big|_{\bar{\Phi}=0}, \quad (\text{A.2})$$

and the flow is characterized by a set of M coupled equations for \bar{g}_{2n} .

- (1) $M = 2$:

At this order, we have

$$\begin{aligned} \bar{\beta}_2 &= -2\bar{g}_2 - \frac{\bar{g}_4}{1 + \bar{g}_2}, \\ \bar{\beta}_4 &= -\bar{g}_4 + \frac{3\bar{g}_4^2}{(1 + \bar{g}_2)^2} + O(\bar{g}_6), \end{aligned} \quad (\text{A.3})$$

and the Wilson-Fisher fixed point is located at $(\bar{g}_2^*, \bar{g}_4^*) = (-\frac{1}{7}, \frac{12}{49})$. Linearizing the flow then yields

$$k \frac{\partial}{\partial k} \begin{pmatrix} \bar{g}_2 \\ \bar{g}_4 \end{pmatrix} = \mathcal{M} \begin{pmatrix} \bar{g}_2 \\ \bar{g}_4 \end{pmatrix}, \quad (\text{A.4})$$

where

$$\mathcal{M} = \begin{pmatrix} \frac{\partial \bar{\beta}_2}{\partial \bar{g}_2} & \frac{\partial \bar{\beta}_2}{\partial \bar{g}_4} \\ \frac{\partial \bar{\beta}_4}{\partial \bar{g}_2} & \frac{\partial \bar{\beta}_4}{\partial \bar{g}_4} \end{pmatrix}_{\bar{g}^*} = \begin{pmatrix} -2 + \frac{\bar{g}_4^*}{(1+\bar{g}_2^*)^2} & -\frac{1}{1+\bar{g}_2^*} \\ -\frac{6\bar{g}_4^{2*}}{(1+\bar{g}_2^*)^3} & -\epsilon + \frac{6\bar{g}_4^*}{(1+\bar{g}_2^*)^2} \end{pmatrix} = \begin{pmatrix} -2 + \frac{\epsilon}{3} & -\frac{6+\epsilon}{6} \\ -\frac{4\epsilon^2}{6+\epsilon} & \epsilon \end{pmatrix} \quad (\text{A.5})$$

is the linearized RG matrix about the Wilson-Fisher fixed point. Upon solving the eigenvalue problem for \mathcal{M} , we find $\nu = 0.527$ which deviates from the exact value 0.689, found by solving the non-truncated equation (A.1). The discrepancy is due to the fact that our approximate Wilson-Fisher fixed point still lies too far away from the exact solution $(s_2, s_4) = (-0.4615, 0.4970)$. Thus in the neighborhood of our approximate solution, higher-order operators continue to evolve and therefore must be included in order to improve the accuracy.

(2) $M = 3$:

Taking into consideration the running of \bar{g}_6 , we have

$$\begin{aligned} \bar{\beta}_2 &= -2\bar{g}_2 - \frac{\bar{g}_4}{1+\bar{g}_2}, \\ \bar{\beta}_4 &= -\bar{g}_4 + \frac{3\bar{g}_4^2}{(1+\bar{g}_2)^2} - \frac{\bar{g}_6}{1+\bar{g}_2}, \\ \bar{\beta}_6 &= -\frac{30\bar{g}_4^3}{(1+\bar{g}_2)^3} + \frac{15\bar{g}_4\bar{g}_6}{(1+\bar{g}_2)^2} + O(\bar{g}_8), \end{aligned} \quad (\text{A.6})$$

which leads to

$$(\bar{g}_2^*, \bar{g}_4^*, \bar{g}_6^*) = \left(-\frac{1}{3}, \frac{4}{9}, \frac{16}{27}\right). \quad (\text{A.7})$$

A comparison with the $M = 2$ calculation shows that the fixed points are now closer to the exact solution with the inclusion of \bar{g}_6 , and hence a more accurate ν is expected. Indeed for $M = 3$ we find $\nu = 0.585$. The complex singularities near the origin at this order are found to be $\bar{\Phi}_c = \pm 0.58998 \pm 2.20183i$, or $(|\bar{\Phi}_c|, \theta_c) = (2.2795, \pm 0.4167\pi)$.

As discussed in Sec. III, the terms from the ϵ expansion are reshuffled in the polynomial truncation scheme. Retaining terms up to $O(\epsilon^3)$ at this order, we find

$$\mathcal{M} = \begin{pmatrix} -2 + \frac{\epsilon}{3} + \frac{5\epsilon^2}{9} + \frac{55\epsilon^3}{54} & -(1 + \frac{\epsilon}{6} + \frac{5\epsilon^2}{18} + \frac{55\epsilon^3}{108}) & 0 \\ -\frac{2\epsilon^2}{3} - \frac{14\epsilon^3}{9} & \epsilon + \frac{10\epsilon^2}{3} + \frac{55\epsilon^3}{9} & -(1 + \frac{\epsilon}{6} + \frac{5\epsilon^2}{18} + \frac{55\epsilon^3}{108}) \\ \frac{10\epsilon^3}{3} & -10\epsilon^2 - \frac{70\epsilon^3}{3} & 2 + 3\epsilon + \frac{25\epsilon^2}{3} + \frac{275\epsilon^3}{18} \end{pmatrix}, \quad (\text{A.8})$$

which, for $\epsilon = 1$, leads to

$$\nu = \frac{1}{2} + \frac{1}{12} \epsilon + \frac{5}{72} \epsilon^2 + O(\epsilon^3), \quad (\text{A.9})$$

or $\nu \approx 0.653$. Comparing Eq. (A.9) with that obtained in [23]

$$\nu' = \frac{1}{2} + \frac{1}{12} \epsilon + \frac{7}{162} \epsilon^2 + O(\epsilon^3), \quad (\text{A.10})$$

we see that they agree up to $O(\epsilon)$; the discrepancy in the ϵ^2 term is due to the negligence of certain Feynman diagrams as well as the wavefunction renormalization.

(3) $M \geq 4$:

With increasing M , our approximate fixed point moves even closer to the non-truncated solution and a greater accuracy is attained. The results are summarized as follows:

M	\bar{g}_2^*	\bar{g}_4^*	\bar{g}_6^*	\bar{g}_8^*	\bar{g}_{10}^*	\bar{g}_{12}^*	\bar{g}_{14}^*	\bar{g}_{16}^*
2	-.1429	.2449	-	-	-	-	-	-
3	-.3333	.4444	.5925	-	-	-	-	-
4	-.4664	.4977	1.1273	2.7804	-	-	-	-
5	-.5163	.4995	1.3056	4.2462	9.9214	-	-	-
6	-.4508	.4952	1.0675	2.3609	-2.303	-77.3326	-	-
7	-.4349	.4915	1.0048	1.9537	-4.2865	-84.4919	-187.96	-
8	-.4665	.49776	1.1278	2.7837	0.0191	-66.3291	248.552	18590.5

Table 1. \bar{g}_n^* as a function of M .

The relation between different \bar{g}_n^* 's can be obtained by expanding \bar{U}^* about $\bar{\Phi} = 0$:

$$\bar{U}^*(\bar{\Phi}) = -\frac{1}{3} \ln(1 + \bar{g}_2^*) + \frac{\bar{g}_2^*}{2} \bar{\Phi}^2 + \sum_{n=2}^{\infty} \frac{\bar{g}_{2n}^*}{(2n)!} \bar{\Phi}^{2n}. \quad (\text{A.11})$$

For large M , the value of \bar{g}_2^* approaches $s = -0.461533$ and \bar{g}_{2n}^* can be rewritten in terms of s as:

$$\begin{aligned} \bar{g}_4^* &= -2s(1+s), \\ \bar{g}_6^* &= 2s(1+s)(1+7s), \\ \bar{g}_8^* &= -60s^2(1+s)(1+3s), \\ \bar{g}_{10}^* &= 40s^2(1+s)(2+43s+83s^2), \\ \bar{g}_{12}^* &= -80s^2(1+s)(-2+45s+549s^2+880s^3), \dots \end{aligned} \quad (\text{A.12})$$

From the non-truncated RG equation we see that the potential becomes singular when the argument inside logarithm vanishes, i.e., $1 + \bar{U}^{*''}(\bar{\Phi}) = 0$. Therefore, when expanding $\ln[1 + \bar{U}^{*''}(\bar{\Phi})]$ in power series of $\bar{\Phi}$, for large enough M and $\bar{g}_2^* \approx s$, one observes a four-fold periodic oscillation of \bar{g}_n^* in $(+, +, -, -)$ pattern, due to the presence of a complex singularity near the origin whose phase is approximately $\pi/2$. Thus, increasing M will at first improve the result by pushing the singularity further away from the origin $\bar{\Phi} = 0$ where the expansion is made, but eventually the series starts to oscillates about $\nu = 0.689 \pm 0.008$.

2. expansion about $\bar{\Phi}^2 \neq 0$:

In order to improve the convergence in polynomial truncation, Aoki *et al* has considered an expansion about some non-vanishing field instead of the origin [13]. Employing $\bar{\chi} = \bar{\Phi}^2/2$ which preserves the Z_2 symmetry of the original action, Eq. (3.1) becomes

$$\left[k \frac{\partial}{\partial k} - (d-2)\bar{\chi} \frac{\partial}{\partial \bar{\chi}} + d \right] \bar{U}_k(\bar{\chi}) = -\ln \left[1 + \bar{U}'_k(\chi) + 2\bar{\chi} \bar{U}''_k(\chi) \right]. \quad (\text{A.13})$$

The expansion

$$\bar{U}_k(\bar{\chi}) = \sum_{n=0}^M \frac{c_n(k)}{n!} (\bar{\chi} - \bar{\chi}'(k))^n, \quad c_n(k) = \bar{U}_k^{(n)}(\chi') = \frac{\partial^n \bar{U}_k}{\partial \bar{\chi}^n} \Big|_{\bar{\chi}=\bar{\chi}'}, \quad (\text{A.14})$$

leads to

$$\begin{aligned} \dot{c}_0 &= \dot{\chi}' c_1 - (4-\epsilon)c_0 + (2-\epsilon)\chi' c_1 - \ln(1 + c_1 + 2\chi' c_2), \\ \dot{c}_1 &= \dot{\chi}' c_2 - 2c_1 - \chi' [(-2+\epsilon)c_2 + 2\hat{c}_3] - 3\hat{c}_2, \\ \dot{c}_2 &= \dot{\chi}' c_3 - (4-\epsilon)c_2 + (2-\epsilon)(2c_2 + \chi' c_3) + (3\hat{c}_2 + 2\chi' \hat{c}_3)^2 - (5\hat{c}_3 + 2\chi' \hat{c}_4), \\ \dot{c}_3 &= \dot{\chi}' c_4 - (4-\epsilon)c_3 + (2-\epsilon)(3c_3 + \chi' c_4) - 2(3\hat{c}_2 + 2\chi' \hat{c}_3)^3, \\ &\quad + 3(3\hat{c}_2 + 2\chi' \hat{c}_3)(5\hat{c}_3 + 2\chi' \hat{c}_4) - 7\hat{c}_4 + O(c^5), \\ \dot{c}_4 &= (4-3\epsilon)c_4 + 6(3\hat{c}_2 + 2\chi' \hat{c}_3)^4 + 28(3\hat{c}_2 + 2\chi' \hat{c}_3)\hat{c}_4 - 12(3\hat{c}_2 + 2\chi' \hat{c}_3)^2(5\hat{c}_3 + 2\chi' \hat{c}_4), \\ &\quad + 3(5\hat{c}_3 + 2\chi' \hat{c}_4)^2 + O(c^5, c^6), \dots \end{aligned} \quad (\text{A.15})$$

where $\hat{c}_n = c_n/(1 + c_1 + 2\chi' c_2)$. As illustrated in Sec. III, a more rapid convergence would be obtained if the expansion is made around or near the minimum $\chi_0 = 1.844$. We summarize in Table 2 below for the results obtained about $\chi' = 2$: From the Table we see a remarkable convergence of ν toward the full LPA solution in this expansion scheme.

M	ν	c_1	c_2	c_3	c_4	c_5	c_6	c_7	c_8	c_9
3	.66781	-.0084	.2664	.0829	-	-	-	-	-	-
4	.68698	.0303	.3343	.1091	.0137	-	-	-	-	-
5	.68803	.0490	.3586	.1155	.0145	-.0071	-	-	-	-
6	.68907	.0512	.3619	.1167	.0151	-.0072	.0016	-	-	-
7	.68956	.0498	.3601	.1162	.0150	-.0066	.0016	.0026	-	-
8	.68952	.0492	.3591	.1159	.0148	-.0067	.0011	.0023	-.0040	-
9	.68948	.0491	.3590	.1159	.0148	-.0066	.0011	.0025	-.0040	.0012

Table 2. The critical exponent ν coupling constants c_n as a function of M .

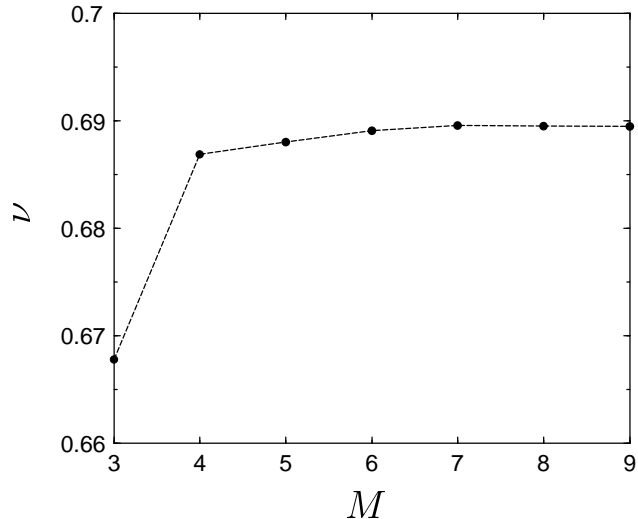


Figure 7. Critical exponent ν as a function of M obtained using the invariant expansion about $\chi'=2$.

APPENDIX B: MODIFIED BLOCKED PROPAGATORS

We have seen that with a smooth cutoff the momentum integrations for the fixed-point solution are divergent in the self-consistent RG formalism, while they remain completely analytic in the LPA. The distinction can be readily understood from the manner in which the propagators are modified in the two approaches.

a. exact RG

In the exact RG approach, the second functional determinant is given by $\tilde{S}_k''[\Phi] = C_k^{-1} + S''[\Phi]$ where $C_k^{-1} = p^2(1 - \tilde{\rho}_{k,\sigma})/\tilde{\rho}_{k,\sigma}$. This in turn implies a modified (dimensionless) propagator of the form

$$\Delta_\sigma(z) = \frac{1}{P_\sigma^2(z) + \bar{g}_2}, \quad (\text{B.1})$$

where $z = p/k$, $P_\sigma^2(z) = z^2/\tilde{\rho}_{k,\sigma}$ and $\bar{g}_2 = \bar{U}_k''(0)$. Let us first examine the behavior of $P_\sigma^2(z)$. For definiteness we take the smooth smearing functions to be $\tilde{\rho}_b(z) = 1 - e^{-az^b}$ as considered in Sec. IV.

We see that as z is decreased, with the exception of $b = 2$, P_b^2 attains a minimum and then diverges as $z \rightarrow 0$. The minimum z_0 , located by $\partial P_b^2/\partial z = 0$, satisfies the relation $z_0^b e^{-az_0^b}/(1 - e^{-az_0^b}) = 2/ab$ and implies a minimum $P_b^2(z_0) = 2z_0^{2-b} e^{az_0^b}/ab$. As can be seen from Table 3, $P_b^2(z_0)$ approaches unity in the limit $b \rightarrow \infty$. As recently addressed by Litim [15], b can be chosen in such a way as to achieve the maximum radius of convergence $R = \lim_{n \rightarrow \infty} a_n/a_{n+2}$ in the amplitude expansion whose coefficients are given by

$$a_n = - \int_0^\infty dz z^{d+1} \left(k \frac{\partial \tilde{\rho}_{k,\sigma}(z)}{\partial k} \right) P_\sigma^{-n}(z). \quad (\text{B.2})$$

By using the following criterion [15]:

$$R_{\text{opt}} = \max \left(\min_{z \geq 0} P_\sigma^2(z) \right), \quad (\text{B.3})$$

the optimal smoothness parameter associated with this particular class of smearing functions is given by $b_{\text{opt}} = 2/\ln 2$, with $R_{\text{opt}} = 2$. On the other hand, based on the principle of minimum sensitivity, it was found that $b^* = 3$ yields the fastest rate of convergence with respect to polynomial expansion for ν [14]. We emphasize that the two optimization procedures are inherently different; while b_{opt} is a universal result for the exponential smearing function, the value of b^* depends on the model and the physical quantity under study [28].

b	z_0	$P_b^2(z_0)$
2	0	$1/\ln 2 = 1.4427$
$2/\ln 2$	1	2
3	1.0324	1.9974
4	1.1603	1.8821
5	1.1849	1.7508
20	1.0861	1.2122

Table 3. Location of the minimum of P_b^2 as a function of b .

One may also consider the power-law cutoff $\tilde{\rho}_m(z) = z^m/(1+z^m)$. From Table 4 we may readily conclude that $m_{\text{opt}} = 4$. The minimum sensitivity condition utilized in Ref. [14] gives $m^* = 5.5$.

m	$z_0 = (\frac{m-2}{2})^{1/m}$	$P_m^2(z_0) = (\frac{m-2}{2})^{2/m} (\frac{m}{m-2})$
2	0	1
3	.7937	1.8899
4	1	2
5.5	1.1071	1.9261
20	1.1161	1.3841

Table 4. Location of the minimum of P_m^2 as a function of m .

In Fig. 8 the blocked propagator is depicted for the exponential cutoff. Note that for $b = 2$, $1/P_b^2(z)$ acquires an effective mass which remains finite in the limit $z \rightarrow 0$.

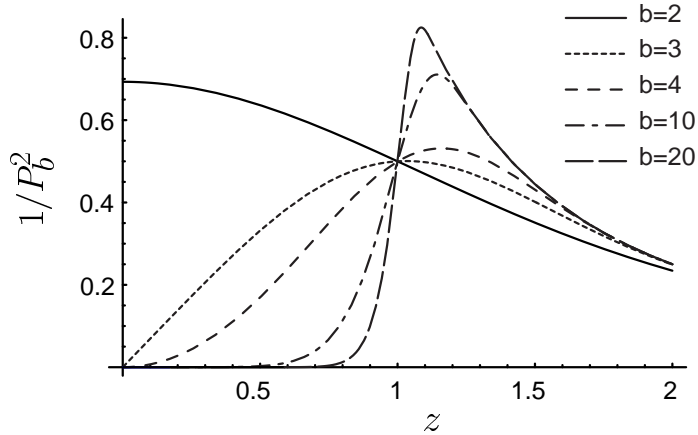


Figure 8. $1/P_b^2(z)$ as a function of z with $a=\ln 2$ and $b=2,3,4,10,20$. The propagator is IR finite as $z\rightarrow 0$.

Let us now consider the effect of \bar{g}_2 . In the symmetric phase where $\bar{g}_2 > 0$, the change is only a shift $P_b^2 \rightarrow P_b^2 + \bar{g}_2$. On the other hand, if $\bar{g}_2 < 0$ as in the case of spontaneous symmetry breaking or during the course of RG evolution where \bar{g}_2 is still negative, the modified propagator can become singular if $P_b^2(z) + \bar{g}_2 \leq 0$. However, this does not happen in LPA where $-\bar{g}_2^* = 0.461533 < \min P_b^2(z) = 1$. Thus in the LPA prescription with a smooth cutoff, the momentum integrations are completely analytic. We comment that in the case of spontaneous symmetry breaking where \bar{g}_2 remains negative down to $k = 0$, one expects the inverse (dimensionful) propagator $(p^2/\tilde{\rho}_b) + g_2$ to vanish at some scale k_{cr} , and the region below $k < k_{\text{cr}}$ becomes inaccessible by conventional perturbation theory.

b. self-consistent RG

Let us now turn to the self-consistent RG prescription. In this formalism, the modified propagator reads

$$\Delta_\sigma(z) = \frac{\tilde{\rho}_\sigma(z)}{z^2 + \bar{g}_2}. \quad (\text{B.4})$$

Contrary to Eq. (B.1), \bar{g}_2 is also influenced by the presence of $\tilde{\rho}_\sigma(z)$ and must not be treated separately. Using the exponential smearing function $\tilde{\rho}_b(z)$ as an example, we find that for $\bar{g}_2 > 0$ the qualitative feature of the modified propagator remains the same except for $b = 2$; while P_b^2 approaches $1/\ln 2$ as $z \rightarrow 0$ in the exact RG formalism, it diverges in the self-consistent RG prescription. The minimum of $\tilde{P}_b^2(z)$ is located by solving

$$\frac{z_0^2 + \bar{g}_2}{1 - e^{-az_0^b}} = \frac{2z_0^{2-b} e^{az_0^b}}{ab}. \quad (\text{B.5})$$

The major difference between the two schemes occurs when $\bar{g}_2 < 0$. As shown in Fig. 9 below, while the propagator in the former remains analytic (for $\bar{g}_2 > -1$), singularity is

present in the latter. Thus, when employing the self-consistent RG prescription to analyze the fixed-point solution, it is desirable to expand about some $\bar{\Phi}_0$ where $\bar{U}_k''(\bar{\Phi}_0) > 0$.

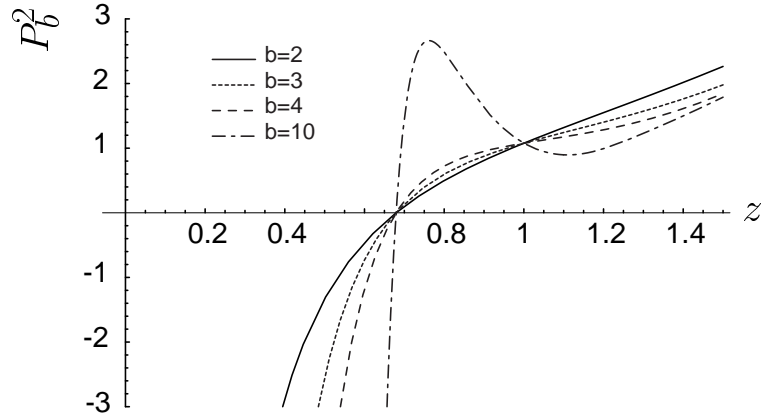


Figure 9. $\tilde{P}_b^2(z)$ as a function of z with $a=\ln 2$ and $b=2,3,4$ and 10 for $\bar{g}_2=-0.461533<0$. The inverse propagator becomes singular when $z\leq\sqrt{-\bar{g}_2^*}$.

APPENDIX C: ASYMPTOTIC EXPANSION WITH SMOOTH SMEARING

In Sec. IV we see that the momentum integrations for the fixed-point solution in the self-consistent RG are divergent due to the negative fixed-point value \bar{g}_2^* . Since $\bar{g}_2^* \approx -0.4615$ is a “small” negative number, we inquire how good the approximation is to make an asymptotic expansion about $\bar{g}_2^* = 0$.

To explore the asymptotic limit, we first expand $U^*(\bar{\Phi})$ about the origin, and the $\bar{\beta}$ functions read

$$\begin{aligned}\bar{\beta}_2 &= -2\bar{g}_2 - \bar{g}_4 I_1 \\ \bar{\beta}_4 &= -\epsilon\bar{g}_4 + 3\bar{g}_4^2 I_2 - \bar{g}_6 I_1 \\ \bar{\beta}_6 &= (2d-6)\bar{g}_6 - 30\bar{g}_4^3 I_3 + 15\bar{g}_4\bar{g}_6 I_2 - \bar{g}_8 I_1, \dots\end{aligned}\tag{C.1}$$

where

$$I_n(\bar{g}_2) = \int_0^1 dt \frac{z^d(t)}{[z^2(t) + \bar{g}_2]^n} = \int_0^1 \frac{dz z^{d-1} (abz^b e^{-az^b})}{(z^2 + \bar{g}_2)^n} = - \int_0^1 \frac{dz z^{d-1}}{(z^2 + \bar{g}_2)^n} \left(k \frac{\partial \tilde{\rho}_{k,b}}{\partial k} \right).\tag{C.2}$$

At $M = 2$ the 2×2 linearized RG matrix becomes

$$\mathcal{M}_b = \begin{pmatrix} -2 + \bar{g}_4^* I_2(\bar{g}_2^*) & -I_1(\bar{g}_2^*) \\ -6\bar{g}_4^{*2} I_3(\bar{g}_2^*) & -\epsilon + 6\bar{g}_4^* I_2(\bar{g}_2^*) \end{pmatrix},\tag{C.3}$$

where the non-trivial Wilson-Fisher fixed points are located by solving the transcendental equations

$$0 = 6\bar{g}_2^* I_2(\bar{g}_2^*) + \epsilon I_1(\bar{g}_2^*) = \int_0^1 dt \frac{z^d(t) [(6+\epsilon)\bar{g}_2^* + \epsilon z^2(t)]}{(z^2(t) + \bar{g}_2^*)^2},\tag{C.4}$$

and $\bar{g}_4^* = \epsilon/3I_2(\bar{g}_2^*)$. Note that in the limit $b \rightarrow \infty$, $I_n \rightarrow (1+\bar{g}_2)^{-n}$, and we readily recover the sharp cutoff results.

Expanding $I_n(\bar{g}_2)$ about $\bar{g}_2 = 0$:

$$\begin{aligned} I_n(\bar{g}_2) &= ab \int_0^\infty \frac{dz z^{d-1+b-2n} e^{-az^b}}{\left[1 + (\bar{g}_2/z^2)\right]^n} \\ &= \sum_{i=0}^{\infty} (-\bar{g}_2)^i \binom{i+n-1}{n-1} a^{-\frac{d-2(i+n)}{b}} \Gamma\left(\frac{b+d-2(i+n)}{b}\right), \end{aligned} \quad (\text{C.5})$$

we have for $\epsilon = 1$,

$$(\bar{g}_2^*, \bar{g}_4^*) = \left(\frac{5c_1 - \sqrt{25c_1^2 + 44c_0c_2}}{22c_2}, \frac{6c_1 - \sqrt{25c_1^2 + 44c_0c_2}}{3(c_1^2 - 4c_0c_2)} \right), \quad (\text{C.6})$$

and

$$\mathcal{M}_b = \begin{pmatrix} -\frac{5}{3} & \frac{3(5c_1^2 - 44c_0c_2 - c_1\sqrt{25c_1^2 + 44c_0c_2})}{121c_2^2} \\ -\frac{2c_2(-6c_1 + \sqrt{25c_1^2 + 44c_0c_2})^2}{3(c_1^2 - 4c_0c_2)^2} & 1 \end{pmatrix}, \quad (\text{C.7})$$

where $c_0 = a^{-1/b}\Gamma(1+1/b)$, $c_1 = a^{1/b}\Gamma(1-1/b)$, and $c_2 = \Gamma(1-3/b)$. The b dependence of the exponent ν is depicted in Fig. 10 below. From the Figure, we see that the expansion is only reliable for sufficiently large b . Indeed as $b \rightarrow \infty$, ν approaches 0.525 which is the sharp cutoff result for $M = 2$.

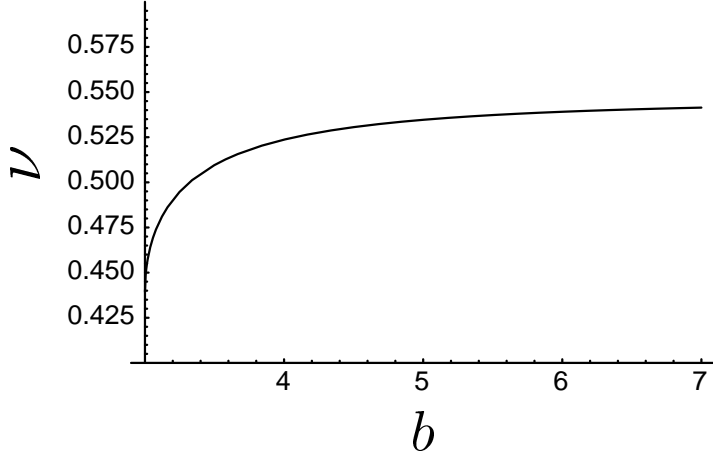


Figure 10. Asymptotic value of ν as a function of b .

The asymptotic limit with $\tilde{\rho}_{k,m} = \frac{(p/k)^m}{1+(p/k)^m}$ can be explored in a similar manner. In this case we have

$$I_n(\bar{g}_2) = - \int_0^\infty \frac{dz z^{d-1}}{(z^2 + \bar{g}_2)^n} \left(k \frac{\partial \tilde{\rho}_{k,m}}{\partial k} \right) = m \int_0^\infty \frac{dz z^{d+m-1}}{(z^2 + \bar{g}_2)^n (1+z^m)^2}, \quad (\text{C.8})$$

and the fixed-point solution for $M = 2$ is found by solving

$$0 = 6\bar{g}_2^* I_2(\bar{g}_2^*) + \epsilon I_1(\bar{g}_2^*) = m \int_0^\infty \frac{dz z^{m+2} (7\bar{g}_2^* + z^2)}{(1 + z^m)^2 (z^2 + \bar{g}_2^*)^2}. \quad (\text{C.9})$$

Making an asymptotic expansion, we have

$$I_n(\bar{g}_2) = \sum_{i=0}^{\infty} (-\bar{g}_2)^i \binom{i+n-1}{n-1} \frac{\pi(d-2(i+n))}{m} \csc\left(\frac{\pi(d-2(i+n))}{m}\right), \quad (\text{C.10})$$

provided that $d - 2(i+n) + m > 0$. The resulting linearized RG matrix takes on the same form as Eq. (C.7), where $c_0 = c_1 = \frac{\pi}{m} \csc(\frac{\pi}{m})$ and $c_2 = 3\frac{\pi}{m} \csc(\frac{3\pi}{m})$. The m dependence of ν is shown in Fig. 11. Once more, the results are only reliable in the large m limit, where $\nu \approx 0.525$, in agreement with that obtained using the sharp cutoff.

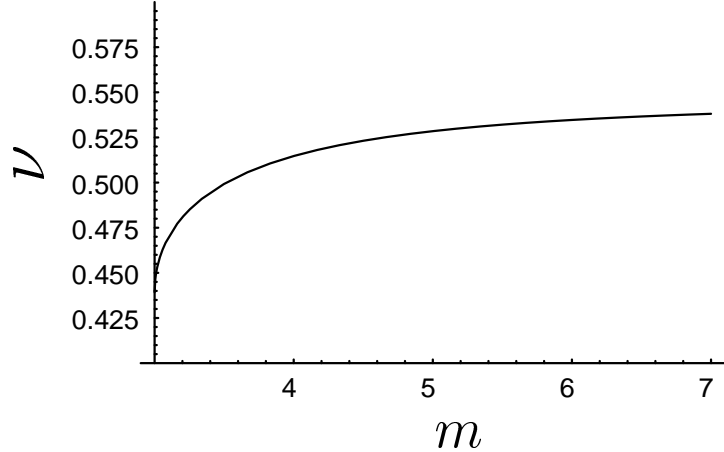


Figure 11. Critical exponent ν as a function of m .

REFERENCES

- [1] K. Wilson, *Phys. Rev.* **B4** (1971) 3174; K. Wilson and J. Kogut, *Phys. Rep.* **12C** (1975) 75.
- [2] F.J. Wegner and A. Houghton, *Phys. Rev* **A8** (1972) 401.
- [3] J. Polchinski, *Nucl. Phys.* **B231** (1984) 269.
- [4] T. R. Morris, *Phys. Lett.* **B334** (1994) 355 and **B329** (1994) 241;
- [5] see, for example, J. Berges, N. Tetradis and C. Wetterich, hep-ph/0005122 and references therein.
N. Tetradis and C. Wetterich, *Nucl. Phys.* **B422** (1994) 541;

B. Bergerhoff and J. Reingruber, *Phys. Rev.* **D60** (1999) 105036;
 B. Bergerhoff, J. Manus, J. Reingruber, *ibid.* **D61** (2000) 125005;
 B. Bergerhoff, *Phys. Lett.* **B437** (1998) 381;
 [6] C. Bagnuls and C. Bervillier, hep-th/0002034.
 J. Comellas and A. Travesset, *Nucl/ Phys.* **B498** (1997) 539.
 [7] T. R. Morris, *Int. J. Mod. Phys.* **A9** (1994) 2411; *Nucl. Phys.* **B509** (1998) 637 and **B495** (1997) 477, and references therein.
 [8] S.-B. Liao and J. Polonyi, *Ann. Phys.* **222** (1993) 122 and *Phys. Rev.* **D51** (1995) 4474.
 [9] J. F. Nicoll, T. S. Chang and H. E. Stanley, *Phys. Rev. Lett.* **32** (1974) 1446, **33** (1974) 540; *Phys. Rev.* **A13** (1976) 1251.
 [10] S.-B. Liao and M. Strickland, *Nucl. Phys.* **B497** (1997) 611 and *ibid.* **B532** (1998) 753.
 [11] A. Hasenfratz and P. Hasenfratz, *Nucl.* **B270** (1986) 687.
 [12] A. Margaritis, G. Odor and A. Patkos, *Z. Phys.* **C39** (1988) 109.
 [13] K. Aoki, K. Morikawa, W. Souma, J. Sumi and H. Terao, *Prog. Theor. Phys.* **95** (1996) 409 and **99** (1998) 451.
 [14] S.-B. Liao, J. Polonyi and M. Strickland, *Nucl. Phys.* **B567** (2000) 493.
 [15] D. Litim, *Phys. Lett.* **B486** (2000) 92.
 [16] S.-B. Liao, J. Polonyi and D. P. Xu, *Phys. Rev.* **D51** (1995) 748;
 S.-B. Liao and M. Strickland, *ibid.* **D52** (1995) 3653.
 [17] J. Alexandre and J. Polonyi, hep-th/9902144.
 [18] V. Branchina, *Phys. Rev.* **D62** (2000) 065010;
 A. Bonanno, V. Branchina, H. Mohrbach and D. Zappala, *ibid.* **D60** (1999) 065009;
 A. Bonanno and D. Zappala, *ibid.* **D57** (1998) 7383.
 [19] M. Strickland, Ph.D. thesis and hep-ph/9809592.
 [20] see, for example, K. Aoki, K. Takagi, H. Terao and M. Tomoyose, hep-th/0002038 and references therein.
 [21] O. Bohr, B.-J. Schaefer and J. Wambach, hep-ph/0007098.
 [22] J. Alexandre, V. Branchina and J. Polonyi, *Phys. Rev.* **D58** (1998) 016002.
 [23] J. Zinn-Justin, *Quantum Field Theory and Critical Phenomena*, 3rd ed. (Clarendon, Oxford, 1996).
 [24] J. O. Andersen and M. Strickland, cond-mat/9808346 and cond-mat/9811096.
 [25] G. Papp, B.-J. Schaefer, H.-J. Pirner and J. Wambach, *Phys. Rev.* **D61** (2000) 096002.
 [26] S.-B. Liao, *Phys. Rev.* **D53** (1996) 2020, and *ibid.* **D56** (1997) 5008.
 [27] S.-B. Liao, C.-Y. Lin and M. Strickland, in preparation.
 [28] D. Litim, private communication.